

**A Prospective:  
Quantitative Scanning Tunneling Spectroscopy of Semiconductor Surfaces**

R. M. Feenstra<sup>\*</sup>

Dept. Physics, Carnegie Mellon University, Pittsburgh, Pennsylvania, USA

**Abstract**

Analysis methods that enable quantitative energies of states to be obtained from vacuum tunneling spectra of semiconductors are discussed. The analysis deals with the problem of tip-induced band bending in the semiconductor, which distorts the voltage-scale of the spectra so that it does not correspond directly to energy values. Three-dimensional electrostatic modeling is used to solve the electrostatics of the tip-vacuum-semiconductor system, and an approximate (semiclassical in the radial direction) solution for the wavefunctions is used to obtain the tunnel current. Various applications of the method to semiconductor surfaces and other material systems are discussed, and possible extensions of the method are considered.

---

<sup>\*</sup> corresponding author: feenstra@cmu.edu

Since its inception more than 25 years ago, the scanning tunneling microscopy (STM) has developed into one of the most powerful and versatile tools for surface science.<sup>1</sup> Much of the early work with the STM focused on semiconductor surfaces, whose geometric structures at that time were not fully understood. A variety of spatially-resolved spectroscopic methods were implemented,<sup>2</sup> known collectively as scanning tunneling spectroscopy (STS). Surface electronic states typically in the range  $\pm 2$  eV from the Fermi energy were observed, with the spatial dependence of these states providing definitive information on the underlying geometric arrangement of the atoms. Since then, many other applications of STM/STS on semiconductors have been developed, including *cross-sectional* STM (XSTM) of semiconductor heterostructures.<sup>3</sup> Most recently, low-temperature STS on semiconductors has enabled detailed studies of isolated substitutional impurities on surfaces<sup>4,5,6</sup> as well as transport limitations of carriers in the semiconductor itself.<sup>7</sup>

Over the past decade, much work has been performed to enable *quantitative* interpretation of tunneling spectra of semiconductors.<sup>8,9,10,11,12,13,14,15,16</sup> What makes this task difficult? Primarily the fact that the semiconductor acts as a dielectric, with some of the applied voltage between sample and tip being dropped within the semiconductor itself, as pictured in Fig. 1(a). This occurrence of *tip-induced band bending* leads to shifts in the observed voltage of spectral features, and these shifts must be accounted for in order to derive fundamental energies from the features. In the absence of this band bending, the energy  $E$  of a state can be related to the sample voltage  $V$  at which it is observed by the expression  $E - E_F = eV$ , where  $E_F$  is the Fermi energy. In the presence of tip-induced band bending, this expression for the case of *surface states* is modified to read

$$E - E_F = eV - \phi_0 \quad (1)$$

where  $\phi_0$  is the band bending at the surface, shown in Fig. 1(a). It turns out that to obtain a realistic estimate of  $\phi_0$ , 3-dimensional (3D) finite-element models are required in order to determine the electrostatics of the tip-vacuum-semiconductor system.

For *bulk states*, the situation is more complicated, as pictured in Figs. 1(b) and (c). Now the wavefunction can tail through a forbidden region of the semiconductor (e.g. the depletion region, Fig. 1(b)) and contributions from the wavefunction tailing must be included in any interpretation of the spectra. Thus, a simple *energy alignment* analysis as exemplified by Eq. (1) is insufficient, and one needs a complete *line-shape analysis* of the spectra. In cases of semiconductor accumulation (Fig. 1(c)) or inversion, the situation is even more complicated, and a full self-consistent solution for the quantum states in the semiconductor is needed in order to interpret the observed spectra.

Despite the effort involved, STS analysis along the lines described above can yield significant benefits. Band gaps (surface or bulk) can be quantitatively determined,<sup>13</sup> as can band offsets in semiconductor heterojunctions.<sup>15</sup> The energy of any particular spectral feature can be quantified so long as there are a sufficient number of *known* features in the spectrum to enable evaluation of the parameters in the analysis. Additionally, forces and capacitance between the tip and the surface (or particular charges on a surface) can be

evaluated. Especially where lateral forces are involved, a 3D electrostatics solution is essential, and this type of application has relevance not only for semiconductors but also for metallic surfaces and/or thin insulating films on metals. In this article, a description is given of the tools needed to perform this type of analysis, an example is provided of their utilization, and some possible future applications are discussed.

Before proceeding with a description of the analysis methods, it is worthwhile to mention a few experimental constraints in STS of semiconductors. First and foremost, the properties of the probe-tip can influence the quality of the spectra. Tip cleaning and/or tip formation on a metallic surface prior to the experiment are essential. Reproducing STS observations with different tips is also necessary in order to establish that the results truly reflect the sample rather than some aspect of the tip itself. Another constraint involves the dynamic range of the tunnel current. At least 3 – 4 orders of magnitude in dynamic range are necessary in order to fully define band edges and/or discern weak states within the bandgap. Given the finite integration times available in the measurement (at least at room temperature), a practical method for achieving this range is to vary the tip-sample separation during the measurement, moving the tip towards the surface at the voltage approaches zero from one side and withdrawing it as the voltage increases on the other side of zero.<sup>17</sup> Subsequent normalization of the conductance, either to constant-separation or in the form  $(dI/dV)/(I/V)$ , allows one to remove most of the variable-separation effect and thus meaningfully compare data from different experimental runs.<sup>17</sup>

The computations needed for quantitative STS analysis can be divided into two steps: obtaining the potential from Poisson's equation and obtaining the tunnel current from a solution to Schrodinger's equation. In situations of accumulation or inversion, where self-consistency is important, one iterates between these two steps. The electrostatics solution can be achieved with a 3D finite-element technique.<sup>18</sup> For a hyperbolic-shaped probe tip near a *metallic* sample, the resulting potential distribution in the vacuum is obtained trivially using prolate spheroidal coordinates. Use of these same vacuum coordinates, together with variable-size grids both in the radial direction and into the semiconductor, permits an efficient finite-element solution for a *semiconducting* sample.<sup>12</sup> The nonlinear situations encountered in inversion, accumulation, or in the presence of surface charge densities can also be efficiently handled.<sup>7</sup> The main parameters in the computation are the tip radius of curvature  $R$ , the sample-tip spacing  $s$ , and the potential difference between the tip and a point deep inside the semiconductor (the latter is given by  $eV$  plus the contact potential  $\Delta\phi$ , with the contact potential being the work function difference between tip and sample). Figure 2 illustrates a typical potential distribution for a doped semiconductor without any surface states.<sup>14</sup>

Solution of the Schrodinger equation is more complicated, and in general involves some approximations. A full first-principles solution that includes a tip-induced electric field in the semiconductor has not been attempted by any workers; rather, simplified models using effective-mass bands to describe the semiconductor have been used to date.<sup>8,14,19</sup> Even within such a simple model, solution of the Schrödinger equation is nontrivial. The problem is nonseparable in the  $r$ - and  $z$ -coordinates (perpendicular and parallel to the central axis, respectively), and use of a plane-wave expansion would involve an

impractical number of basis states to describe both the long-range and short-range parts of the wavefunctions in 3D. It should be noted that the goal is to develop a theory that can be routinely used by many users, and one that permits numerous evaluations of the tunnel current as needed for fitting of the experiment to theory. Values for  $R$ ,  $s$ , and  $\Delta\phi$  are determined by such fitting. Values of these parameters are not themselves usually of great interest in the problem, but rather, they serve merely to provide a numerical model with which to extract additional parameters that *are* of interest, such as a band gap, a band offset, or an energy location of some particular surface or bulk state.

For specific potential distributions between tip and sample, variational wavefunctions can be constructed.<sup>7,8</sup> However, this method is problematic to apply to a general solution of the Schrödinger equation over a range of sample-tip voltages (i.e. as is needed for simulation of an entire current vs. voltage curve). For that case, a useful method is to consider only the potential along the central axis of the problem,  $r = 0$ , and then to incorporate that in a planar tunneling problem.<sup>14,16</sup> States of this one-dimensional (1D) potential can be easily obtained by numerical integration. The total wavefunction is separable for this planar geometry, with the radial portion given simply by plane waves. A sum over all states is performed to obtain the tunnel current. This method of solution is valid for potentials that vary relatively slowly in the radial direction (i.e. the radial variation of the potential is being treated *semi-classically*), which is a reasonable approximation for the tip radii encountered in typical situations.<sup>9</sup> This same method can be extended to provide *charge densities* in the semiconductor, as needed for situations of accumulation or inversion.<sup>16</sup> Figure 3 displays a few conduction band states for an n-type semiconductor in accumulation.<sup>16</sup>

As an example of quantitative STS analysis, let us consider the spectrum shown in Fig. 4 obtained from a Ge(111)-c(2x8) surface.<sup>13</sup> The bands centered around  $-1.0$  V and  $+0.7$  V arise from the *rest atoms* and *adatoms* on the surface, respectively.<sup>20, 21, 22, 23</sup> The former band is completely resonant (overlapping in energy) with the valence band (VB), but the latter extends well into the bulk band gap region. The energy difference between the top of the valence band (at  $-0.11$  V) and the bottom of the adatom band (at  $+0.50$  V) gives the surface band gap of the material. From the voltages just mentioned one would estimate a value of 0.61 eV for this gap, but evaluation of tip-induced band bending is needed in order to obtain a more quantitative value. This evaluation is achieved by comparing *known* features in the spectrum with electrostatic computations, thus determining the unknown parameters in the computations including  $R$ ,  $s$ , and  $\Delta\phi$ . Then, by interpolation, the gap can be obtained.

A simplified view of this analysis is shown in Fig. 5. Three of the features in the spectrum of Fig. 4 have known energy – the rest-atom band, the top of the VB, and the linear onset of the bulk conduction band.<sup>13</sup> From these energies, together with the observed voltages of the features, the band bending is deduced from Eq. (1). Additionally, the observed voltage at which inversion of the surface occurs can, with use of the electrostatic theory, yield the band bending. These band bending values are then plotted as a function of voltage, Fig. 5, and the results compared with electrostatic

computations. Then, with the observed voltage of the lower edge of the adatom band being  $+0.50\text{ V}$ , the band bending  $\phi_{0,A}$  at this voltage is found to be about  $0.02 - 0.04\text{ eV}$ . The Fermi energy for this sample is  $0.01\text{ eV}$  above the VB maximum, thus yielding a surface gap of  $\approx 0.48\text{ eV}$ . However, since this analysis utilizes Eq. (1), it has been implicitly assumed that all relevant states are localized near the surface. This is certainly true for the adatom band, and likely true for the rest atom band, but the VB states probably are *not* significantly localized at the surface. A somewhat complex analysis is needed to correct for this (i.e. evaluating for bulk-like states the difference in their shift under the influence of band bending compared to that of a surface state).<sup>13</sup> The result of that analysis produces a refined value for the surface band gap of  $0.49 \pm 0.03\text{ eV}$ .

The above example reveals one limitation in the current analysis method – the need to assume either purely surface or bulk character of the states being treated. Of course, full knowledge of the local density of states of a surface would eliminate this distinction, but that knowledge is not necessarily available for an arbitrary surface under study. The present theory can handle full line-shape analysis of effective-mass bulk states, as pertains to XSTM studies, and surface states can be treated in a limited sense by Eq. (1), but models that handle varying degrees of surface localization have yet to be developed.

Many other limitations of the theory exist (and are potential topics for future work). Image potentials are presently neglected in the treatment of the vacuum barrier; incorporating this in a consistent manner with the effective-mass treatment of the bulk bands would seem to be nontrivial. Moreover, the effective-mass treatment itself is very approximate, and does not properly treat the boundary conditions for the wavefunction at the surface.<sup>24</sup> A more rigorous derivation is needed for this approximation, perhaps along the lines as that derived in early work for oxide barriers<sup>25</sup> or more recently for semiconductor heterointerface problems.<sup>26</sup> Even with the effective-mass treatment, inclusion of additional bands would be useful (i.e. for handling surface other than the (110) III-V surfaces encountered in XSTM). Returning to the limitations with handling surface states, it should also be noted that even for states well localized at the surface such as the adatom band in Fig. 4, a simple model for the line-shape of that type of band is not currently available.

Additional applications of this type of STS analysis can be envisioned. For semiconductor materials, some of the recent studies of substitutional impurities<sup>4,5,6</sup> have benefitted from the type of electrostatic modeling described above. Further analysis to quantitatively handle the Coulomb potential arising from an individual charge on a semiconductor surface (i.e. together with the tip-induced band bending) could be accomplished by a modest extension to the existing theory. The same types of considerations would be relevant for isolated charges on metallic surfaces, or on thin insulating films on metals. Not only is the potential near such isolated charges of interest, but so too are the force and capacitance between the tip and adsorbate. Detailed 3D electrostatic modeling is necessary to derive those quantities.

In all of the above discussion it has been assumed that the tunneling process is the rate-limiting step in the transport of carriers from the probe-tip to the semiconductor, so that

an "equilibrium" situation exists in which the occupation of carriers in the semiconductor is simply described by a constant Fermi-energy. But in actuality, situations arise (at low temperature, or low doping, or for confined states, etc.) in which transport in the semiconductor itself is somewhat limited.<sup>7,10,11,27</sup> In those cases, a much more complicated theory is needed to describe the distribution of carriers and resulting charge densities on the surface and in the bulk of the semiconductor. Such a theory could prove to be useful in enabling the determination of transport parameters for the carriers, even in nanoscale situations as occur in the STM geometry.

The author gratefully acknowledges the contributions to this work of many colleagues and collaborators, including Yang Dong, Sandeep Gaan, Nobuyuki Ishida, Myung-Ho Kang, Lucian Livadaru, and Gerhard Meyer. This work was supported by the National Science Foundation under grant DMR-0503748 and by the Alexander von Humboldt Foundation.

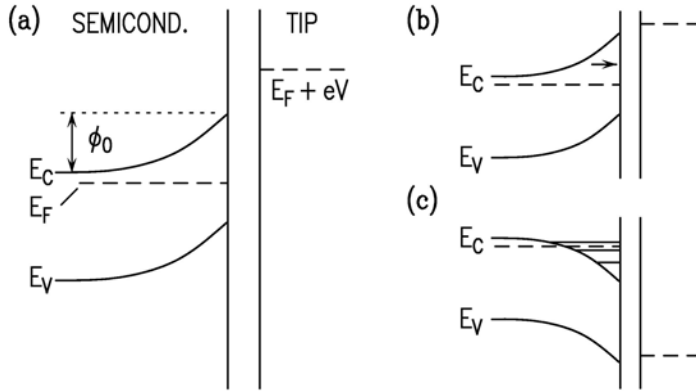


FIG 1. (a) Schematic diagram of energy bands with tip-induced band bending, showing the valence band maximum  $E_V$  and the conduction band minimum  $E_C$ . The sample Fermi level is denoted by  $E_F$  with the tip Fermi level at  $E_F + eV$  where  $V$  is the applied sample-tip voltage bias. The band bending at the surface is denoted by  $\phi_0$ . Quantum effects within the semiconductor are illustrated in (b) and (c) for wavefunction tailing (arrow) through a depletion region and for localized accumulation state formation, respectively.

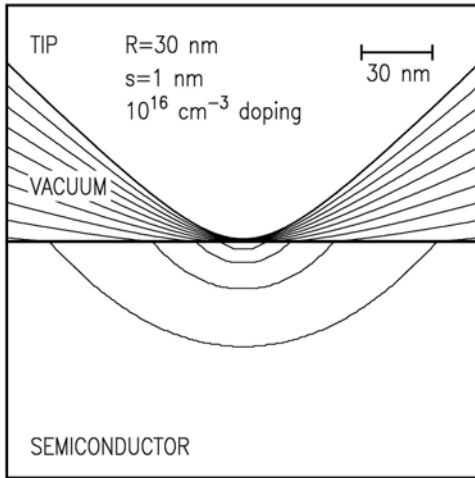


FIG 2. Potential distribution for n-type GaAs in depletion. The potential energy contours shown are separated by one tenth of the potential difference between the tip and a point deep inside the semiconductor.

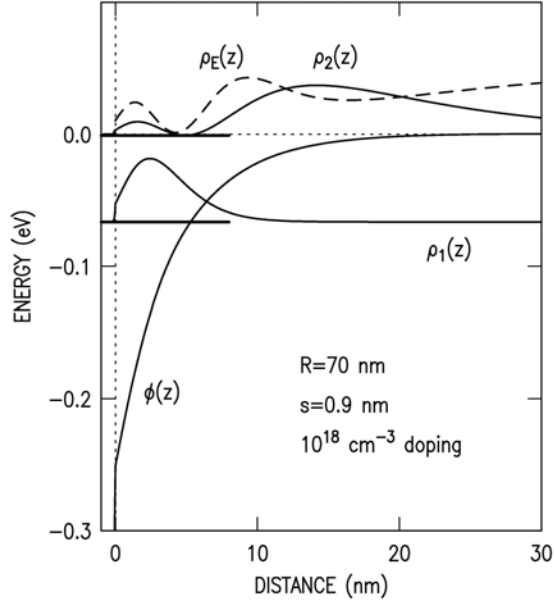


FIG. 3: Electrostatic potential energy  $\phi(z)$ , and energies of localized states (heavy lines) relative to  $E_C$ , for n-type GaAs(110) in accumulation. Also shown are the charge densities of localized accumulation states  $\rho_1(z)$  and  $\rho_2(z)$ , and the charge density of extended states  $\rho_E(z)$  in the conduction band. All quantities refer to their values along the central axis of the problem, and are evaluated at a sample-tip voltage of  $-1.35$  V with contact potential of  $0.43$  eV.

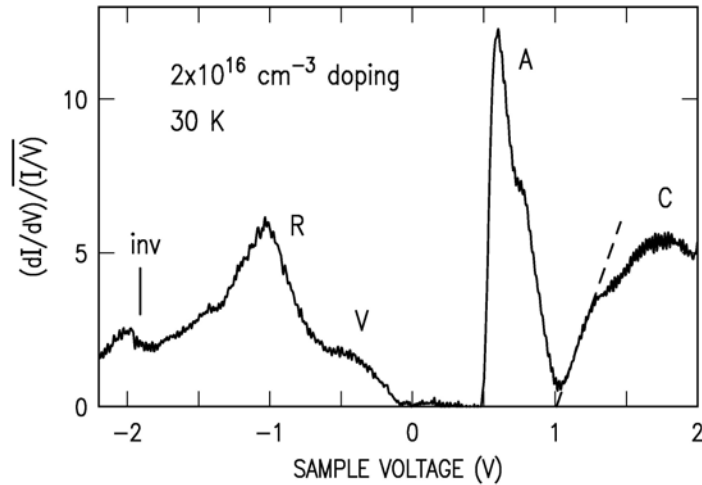


FIG. 4. Tunneling spectrum of the Ge(111)-c( $2 \times 8$ ) surface, showing the rest-atom band (R), top of the valence band (V), adatom band (A), and conduction band (C). The feature marked “inv” arises from inversion of this p-type sample, and the dashed line extending up from  $+1.0$  V marks a linear onset of the bulk conduction band.

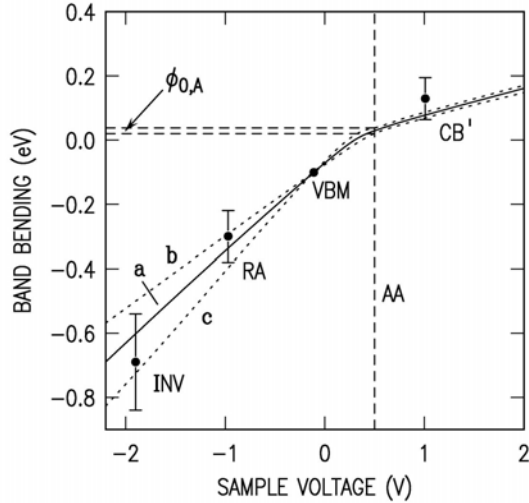


FIG 5. Band bending in the semiconductor at a point opposite the probe tip apex, as a function of sample-tip voltage. Data points are shown for spectral features that have known energy such that the band bending can be absolutely determined (VBM – valence band maximum, RA – peak of rest-atom and, CB' – high lying conduction band feature, and INV – voltage at which inversion occurs). Theoretical curves interpolating between the data points are shown, with the solid line giving an optimal result and the dotted lines giving error bounds. The vertical dashed line is located at the position of the observed onset of the adatom band (AA), with the horizontal dashed lines then giving the band bending at this voltage.

- 
- <sup>1</sup> G. Binnig, H. Rohrer, Ch. Gerber, and E. Weibel, *Phys. Rev. Lett.* **49**, 57 (1983).  
<sup>2</sup> For review, see R. M. Feenstra, *Surf. Sci.* **299/300**, 965 (1994).  
<sup>3</sup> For review, see R. M. Feenstra, *Semicond. Sci. and Technol.* **9**, 2157 (1994).  
<sup>4</sup> D. Kitchen, A. Richardella, Jian-Ming Tang, M. E. Flatte, and A. Yazdani, *Nature* **442**, 7101 (2006).  
<sup>5</sup> F. Marczinowski, J. Wiebe, F. Meier, K. Hashimoto, and R. Wiesendanger, *Phys. Rev. B* **77**, 115318 (2008).  
<sup>6</sup> K. Teichmann, M. Wenderoth, S. Loth, R. G. Ulbrich, J. K. Garleff, A. P. Wijnheijmer, and P. M. Koenraad, *Phys. Rev. Lett.* **101**, 076103 (2008).  
<sup>7</sup> R. M. Feenstra, S. Gaan, G. Meyer and K. H. Rieder, *Phys. Rev. B* **71**, 125316 (2005).  
<sup>8</sup> R. Dombrowski, Chr. Steinebach, Chr. Wittneven, M. Morgenstern, and R. Wiesendanger, *Phys. Rev. B* **59**, 8043 (1999).  
<sup>9</sup> Y. Dong, R. M. Feenstra, R. Hey, and K. H. Ploog, *J. Vac. Sci. Technol. B* **20**, 1677 (2002).  
<sup>10</sup> N. D. Jäger, E. R. Weber, K. Urban, R. Krause-Rehberg, and Ph. Ebert, *Phys. Rev. B* **65**, 195318 (2003).  
<sup>11</sup> N. D. Jäger, E. R. Weber, K. Urban, and Ph. Ebert, *Phys. Rev. B* **67**, 165327 (2003).  
<sup>12</sup> R. M. Feenstra, *J. Vac. Sci. Technol. B* **21**, 2080 (2003).

- 
- <sup>13</sup> R. M. Feenstra, J. Y. Lee, M. H. Kang, G. Meyer, and K. H. Rieder, Phys. Rev. B **73**, 035310 (2006).
- <sup>14</sup> R. M. Feenstra, Y. Dong, M. P. Semtsiv, and W. T. Masselink, Nanotechnology **18**, 044015 (2007).
- <sup>15</sup> Y. Dong, R. M. Feenstra, M. P. Semtsiv and W. T. Masselink, J. Appl. Phys. **103**, 073704 (2008).
- <sup>16</sup> N. Ishida, K. Sueoka, and R. M. Feenstra, accepted for publication in Phys. Rev. B.
- <sup>17</sup> P. Mårtensson and R. M. Feenstra, Phys. Rev. B **39**, 7744 (1989).
- <sup>18</sup> SEMITIP computer program, for 3D band bending and tunnel current computations, available at <http://www.andrew.cmu.edu/user/feenstra/>.
- <sup>19</sup> R. M. Feenstra and J. A. Stroscio, J. Vac. Sci. Technol. B **5**, 923 (1987).
- <sup>20</sup> J. Aarts, A. J. Hoeven and P. K. Larsen, Phys. Rev. B **37**, 8190 (1988), and references therein.
- <sup>21</sup> R. S. Becker, B. S. Swartzentruber, J. S. Vickers, and T. Klitsner, Phys. Rev. B **39**, 1633 (1989).
- <sup>22</sup> F. J. Himpsel, Surf. Sci. Rep. **12**, 1 (1990).
- <sup>23</sup> R. M. Feenstra and A. J. Slavin, Surf. Sci. **251/252**, 401 (1991).
- <sup>24</sup> W. A. Harrison, Phys. Rev. **123**, 85 (1961).
- <sup>25</sup> C. B. Duke, *Tunneling in Solids* (Academic Press, New York, 1969).
- <sup>26</sup> G. Bastard, *Electronic States in Semiconductor Heterostructures*, Solid State Physics, Vol. 44, ed. H. Ehrenreich and D. Turnbull (Academic Press, San Diego, 1991).
- <sup>27</sup> J. Mysliveček, A. Stróžecka, J. Steffl, P. Sobotík, I. Ošt'ádal, and B. Voigtländer, Phys. Rev. B **73**, 161302(R) (2006).